AENSI Journals

Australian Journal of Basic and Applied Sciences

Journal home page: www.ajbasweb.com

Coupled Zno-Fe_3O_4: Nanoparticles Embedded In Polymer Electrolytes: Preparation And Impedance Measurement of The Tin Film

[1]Sanjay Srivastava, Yogesh Srivastav, [2]Vikas Srivastava

[1]*Material Science & Metallurgical Engineering, Maulana Azad National Institute of Technology, Bhopal M.P. (India)-462051*
[2]*TCG Life science Ltd (Chembiotek), Block BN, Plot-7, Sec-V, Salt Lake City, Kolkata, (India) - 700 091*

ARTICLE INFO

Article history:
Received 13 October 2013
Received in revised form 15 January 2014
Accepted 21 January 2014
Available online 1 February 2014

Keywords:
Nano particle, Raman spectra, XRD, Heavy-metal, PVA, SEM, PL Spectra

ABSTRACT

Background: Nanocomposite polymer electrolytes based on poly (vinyl alcohol) (PVA) complexes with lithium-chlorate ($LiClO_4$) and containing mixed ZnO and Fe_2O_3/Fe_3O_4nanoparticles were prepared by the chemical precipitation method, in which the nanoparticles were grown in the host polymer electrolyte. Zinc oxide nanoparticles were synthesized by heating freshly prepared zinc hydroxide (Zn (OH) $_2$) and ferric hydroxide Fe (OH) $_3$from alkaline hydrolysis of $FeCl_3$ solution in different capping agents at 150^{0}C for two hours. The prolonged thermal treatment of the Fe_3O_4 produced Fe_2O_3 hematite nano particle. The thin film of the polymer composite was prepared by a spin coating method. The prepared compound as well as composite was characterized by the X-ray diffraction technique. SEM analysis was used to investigate the surface morphology of the prepared composite. From this investigation, the reinforcing constituents are uniformly distributed in the polymer matrix. The conductivity and impedance of the nanoparticle reinforced polymer matrix were studied by electrochemical impedance spectroscopy (EIS). Ion carriers were formed during nanoparticle addition by $LiClO_4$ precursor. Addition of nano particles in the polymer electrolytes not only improved the ionic conductivity but also improved the performance of the charge carrier, resulting in a maximum conductivity of $1.81x10^{-3}$ S. cm^{-1}. Thin film of the polymer composite shows beautiful results of the impedance, obtained from the EIS investigation.

To Cite This Article: Sanjay Srivastava, Yogesh Srivastav, Vikas Srivastava., Coupled Zno-Fe_3O_4: Nanoparticles Embedded In Polymer Electrolytes: Preparation And Impedance Measurement of The Tin Film ***Aust. J. Basic & Appl. Sci.,*** *7(14): 142-153, 2013*

INTRODUCTION

Solid polymer electrolytes (SPEs), formed by dissolving various useful salts in a polymer solvent, is the most versatile materials for use in rechargeable lithium batteries. Owing to the promising and very wide range of applications in Li secondary batteries, which provide higher output voltage, higher specific capacity, longer cycle life, improved safety, and so on, polymer electrolytes have been increasingly studied in recent decades (Croce *et al*., 19981, Bruno 2001, and Wakihara 2001). For instance, solid polymer electrolyte membranes consisting of poly (2-ethyl-2-oxazoline) (POZ) and $AgBF_4$, or poly (vinyl pyrrolidone) (PVP) and $AgCF_3SO_3$, demonstrated a propylene/propane selectivity of 45 and a total mixed gas presence of 12 GPU (1 GPU = 1×10^{-6} cm^3 (STP) /(cm^2 s cm Hg)) (Hong *et al*.,2001). Polymers including poly (ethylene oxide) (PEO) (Appetecchi *et al*., 2003), polyacrylonitrile (PAN) (Weihua et.al., 2005, Kim *et al*., 2002, Min *et al*., 2003), poly (methyl methacrylate) (PMMA) (Zhang *et al*., 2007), poly (vinylidene fluoride) (PVDF) (Saunier *et al*.,2004), and their copolymers such as poly (acrylonitrile-methyl methacrylate) (PAN-MMA)) (Zhou *et al*., 2010), poly (vinylidene fluoride-co-hexafluoropropylene) (P (VDF-HFP)) (Pasquier *et al*., 2000) have been used as polymer matrixes. However, their ionic conductivity at room temperature is very low and is still inadequate for practical use at higher current densities; despite much research devoted to increasing their ionic conductivity by several orders of magnitude. Recently, solid polymer electrolytes containing inorganic nanoparticles have been demonstrated superior transport properties. For example, conductivity was significantly increased by adding nanoparticles 10% by weight to poly (ethylene oxide) (PEO) /$LiClO_4$ electrolytes (Croce *et al*., 1999). In addition, inorganic nanoparticles such as MnO_2, TiO_2, and ZrO_2 have been used to increase the conductivity of poly aniline composites (Biswas *et al.*, 1999, Su *et al*., 2000, Ray *et al*., 2000). The normal role of inorganic particle fillers in polymer electrolytes is to influence the re-crystallization kinetics of the polymer chain and promote localized amorphous regions, thus enhancing cation transport. Examples of inorganic particles used in polymer composites include SiO_2, Al_2O_3, TiO_2, CdO and ZnO (Agrawal *et al*, 2009). Inorganic particles are also used to enhance the mechanical properties of polymer electrolytes (Ramesh *et al.*, 2001). Depending on the

Corresponding Author: Sanjay Srivastava, Material Science & Metallurgical Engineering, Maulana Azad National Institute of Technology, Bhopal M.P. (India)-462051

characteristics of starting monomer; different preparative methodologies have been adopted to obtain the polymeric materials. They are classified into two major methods, such as electrochemical and chemical polymerization methods. The chemical oxidative polymerization is more applicable than an electrochemical method for the preparation of bulk electrode materials with controllable sizes.

Hence, in the present investigation, the nanoparticles of ZnO and Fe_3O_4 were prepared by the chemical precipitation method but Fe_2O_3prepared by subsequent heating of the precipitate at constant temperature. The polymer nanocomposite was prepared by dispersing the ZnO and Fe_3O_4/Fe_2O_3 in PVA matrix. The synthesized nanoparticles were characterized by FT-IR, UV-Visible spectroscopy, XRD, SEM and electrical conductivity studies. The spin coating method has been used to prepare the thin film of polymer composite.

Experimental:

Material Synthesis:

Zinc oxide was prepared from Zinc hydroxide solution after neutralizing with NaOH. Conventional heating experiments were conducted on a magnetic stirrer for the experiment. On the completion of the reaction, the solid and solution phases were separated by centrifugation and the solids were washed free of salts with de-ionized water thrice followed by ethanol twice. A white colored powder was calcined at 150^0C and then it was grounds for uniformities of the powder. The dry synthetic powders were weighed and the percentage yield was calculated from the expected total amount of ZnO based on the solution concentration and volume and the amount that was actually crystallized.

Magnetic nanoparticles systems analyzed below were prepared by alkaline hydrolysis of highly concentrated solutions of Fe^{2+} and Fe^{3+} salts reported in the Literature (Berger *et al*., 2003). The ferric and ferrous salt solutions were prepared in 2M HCl solvent since the acidic conditions prevent formation of iron hydroxides. The 10 gram of $FeCl_3$ was dissolved in 150 ml of distilled water. 20 ml ammonia solution was added drop by drop into it. The mixture was stirred from the mixer and grinder at 345 rpm for 1 hour under heating in a water bath at 60°C. The mixture was allowed to settle & cooled. The suspensions were finally washed with deionized water to reach approximately 6.5 pH value. After washing, the precipitate 5ml of 25% solution of Perchloric acid (PA – sample) or respectively, citric acid (CA - sample) was added, the resulted dark suspension being further stirred for 1h.The black colored product obtained was washed several times with 20 ml of distilled water each. Then it was washed similarly with 10 ml methanol for 3 times. The obtained product was air dried and weighed. Yield: 0.1999 g.

Reaction:

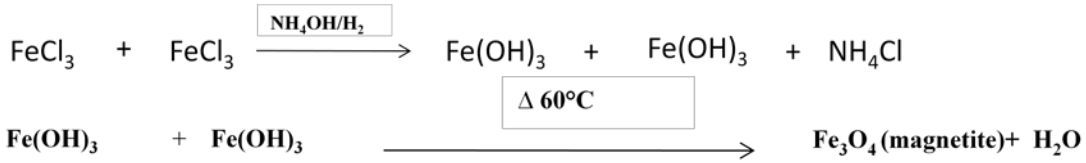

Magnetite nano particles when heated at 300 °C for 4 hours then reddish-brown solid particles was found is hematite nano particles.

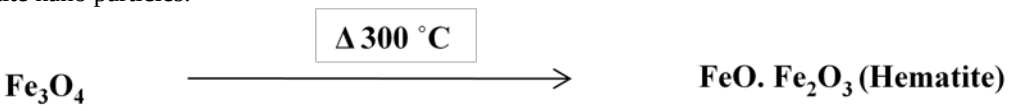

Composite Preparation:

PVA-$LiClO_4$ mixtures were prepared containing 0-10 wt% $LiClO_4$. The PVA and $LiClO_4$ were dissolved in separate solutions. The solutions were mixed at 50^oC for 2 h and evaporated under ambient condition for 5 days to obtain a thin sheet of polymer electrolyte. The polymer composition exhibiting the highest electrical conductivity was prepared from dispersing $Fe_3O_4$and ZnO, nanoparticles. Between volume fraction 0-0.35 v% of $Fe_3O_4$and 0-0.45 v% ZnO, nanoparticles were dispersed in the PVA polymer electrolyte.

Characterization:

Powder X-Ray diffraction of prepared nano sized material was recorded with the help of Rigaku X-ray diffractometer between 10^o to 60^o using CuKα radiation (1.5414Å). The average particle sizes were determined from XRD peak widths employing Debye-Scherrer formula. The UV-Visible spectra of all the solutions were recorded with the help of using Jasco V 500 spectrophotometer in the wavelength region of 200–800 nm. The metallographies specimens were prepared using standard technique and studied under SEM for observing the different feature present in the nanostructure materials as well as in polymer composite.

RESULT AND DISCUSSION

Characterization of ZnO nano Particle:

The synthesis of nanostructures material is a growing area of research. The synthesis of nanostructures by low cost process would be of great technological importance. The ZnO nanostructures were synthesized by co-precipitation methods. In this research work, the ZnO nanoparticles were prepared from zinc hydroxide solution. Based on a fixed proportion, the nanoparticles place inside the deionized water for 72 h, 168h, and 336 h respectively, so as to observe the oxidation and the precipitation status of the nanoparticles. In order to verify the result obtained from the precipitation that the nature of the nanoparticles inside the deionized water will change according to time. The morphology of ZnO that was synthesized from co-precipitation methods was investigated by using an SEM technique. Fig**. 1a** is the SEM image of ZnO nanoparticle after placement of 168 h. As it can be seen that the particles display rod-like form, which indicates the growth of the nanostructures along a certain direction. Its axial length is around 250 nm. It can be clearly seen that the nanoparticles do not have a fixed shape and their distribution is not obvious, but in turn, they become oxidized material clustering and growing irregularly as shown in **Fig 1b**.

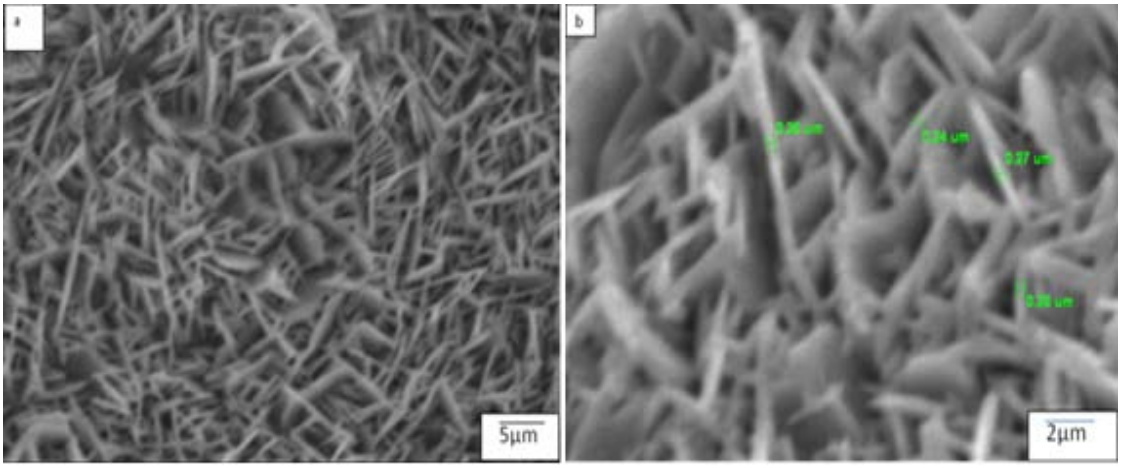

Fig. 1: SEM image of ZnO nanoparticle that is placed in deionized water for 168 h

The XRD patterns of the zinc oxide powders were examined, and are given in **Fig. 2**. The Miller indices of the reflective crystal planes and d-spacing's between them are indicated on the XRD patterns. The strongest characteristic 101 XRD reflection of the Zn (OH) $_2$ crystal in the precursor powder is at 0.7357 nm. Zinc oxide crystal has several XRD reflections. Its characteristic XRD reflections on 0.2807, 0.2596, and 0.2470 nm correspond to 100, 002, and 101 planes, respectively. These reflections match with the wurtzite structural ZnO with lattice constants of a=0.3250 nm and c=0.5207 nm (Croce *et al* 1999, Biswas *et al*., 1999). This structure does not depend on the preparation processes and the morphology of the ZnO powders (Su and kuramoto., 2000, Ray and Biswas 2000, Agrawal *et al* 2009). It is known that the decrease in width of an XRD peak shows the increase in size of the investigated crystal. The relationship between the average crystal size (L) and FWHM in terms of radians is given as follows by the Scherrer formula,

$$L = \frac{0.9\lambda}{(FWHM)\cos\theta} \quad (1)$$

Where λ is the wavelength of the X-rays, FWHM is the full width at half maximum reflection height, and θ is the diffraction angle. The average size of particles in oxide powders was found to be 14-20 NM by using the data for the most characteristic 101 XRD reflections.

Fig 3 shows the Raman spectra of ZnO nanoparticles prepared from co-precipitation technique. Raman measurements were also made using 785nm line of solid state laser; however, the existence of large PL background prevented a quantitative analysis of Raman intensities. The Raman spectra showed the main vibrational bands at 901, 58, 606.5, 481.33, 399.33 and 239.25 cm^{-1}. Wurtzite type ZnO belongs to the C_{6v} (P63mc) space symmetry. Each unit cell is having 4 atoms and occupying 2b sites of symmetry C_{3v}. At the point near the Brillouin zone the following optical phonon modes are allowed, $\Pi_{opt} = A_1+2B_1+E_1+2E_2$. Among these, doubly degenerate B_1 modes are silent, A_1 and E_1 branches are both Raman and infrared active, and other doubly degenerate E_2 modes are Raman active. In the present work we have synthesized ZnO nanoparticles in

the quantum confinement regime. A direct band gap of 3.3 EV in case of bulk ZnO should give rise to an absorption edge at ~375 NM.

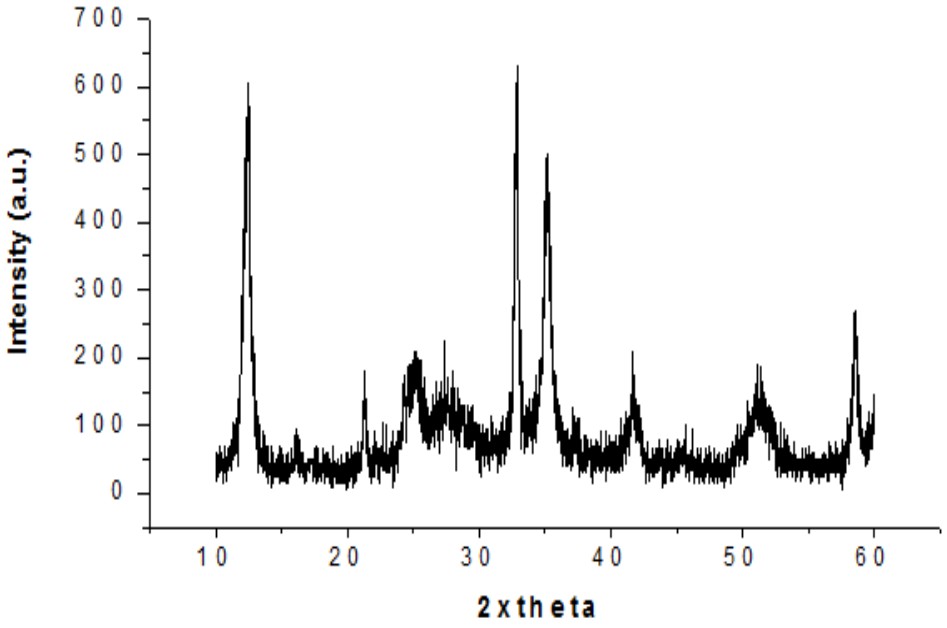

Fig. 2: Typical XRD pattern of the zinc oxide

Fig. 4 shows the optical absorption of ZnO nanoparticles. The absorption spectra demonstrate the absorption peaks around 366 nm (3.23 *eV*) corresponding to the exciton state in the bulk ZnO.Even though these spectra were taken at room temperature, the ZnO nanoparticle samples exhibit salient exciton absorption features due to the relatively large binding energy of the exciton (60 mV).Typical exciton absorption of ZnO nanoparticle at 362 nm is observed in the absorption spectrum at room temperature, which gives blue shifted with respect to the bulk absorption edge appearing at 380nm at room temperature. It is clear that the absorption edge systematically shifts to the lower wavelength or higher energy with decreasing size of the nanoparticle. This pronounced and systematic shift in the absorption edge is due to the quantum size effect. Thus the average particle size can be determined from the inflection point in the absorption vs. wavelength spectrum (Pesika *et al* 2003).

The following Eq. (1), derived by using the effective mass model which describes the size of particles (r, radius) as a function of peak absorbance wavelength (p) for monodispersed ZnO nanoparticles (Pesika *et al* 2003),

$$r(nm) = \frac{-0.3049 + \sqrt{-26.23012 + \frac{10240.72}{\lambda_p(nm)}}}{-6.3829 + \frac{2483.2}{\lambda_p(nm)}} \quad (2)$$

From eq. (1), we have used m_e = 0.26 mo, m_h = 0.59mo, m_o is the free electron mass, ε = 8.5 (dielectric of the medium), and Eg^{bulk} = 3.3 eV. The prepared ZnO nanoparticles form the chemical precipitation route show peak absorbance at 366 NM which corresponds to an average particle size of 15-18 nm. This result is again justified from the XRD investigation.

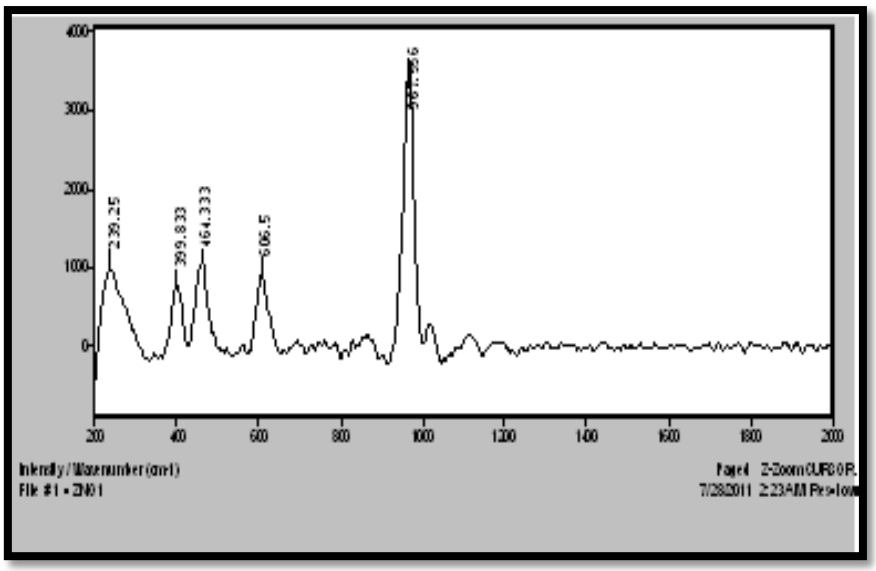

Fig. 3: Raman spectra of ZnO nanoparticles

Fig 5 depicts the photoluminescence spectrum of nanosized ZnO, synthesized in aqueous medium. Strong emission peak centered at 397 nm was observed in ZnO. The ZnO sample exhibits only UV band gap luminescence but no oxygen defect luminescence was observed. The nano powders show an intense violet emission along with the emission in a blue and green band. However, the whole PL emission spectrum covers the 400-700 nm of the visible region of the electromagnetic spectrum. Average position of the most intense peak lies in the violet band in the range 417-424 nm. Blue emission band occurs in the range (a) 447-455 nm (Band-I) (b) 485-486 nm (Band-II). Generally, a green–yellow emission, it is observed around 530 nm, i.e. green– yellow emission as shown in **Fig 5.** In the photoluminescence (PL) spectra of ZnO, typically there are emission bands in the UV and visible regions. The UV peak is usually considered as the characteristic emission of ZnO and attributed to the band edge emission or the exciton transition.

Characterization of Fe_3O_4nano material:

The formula for magnetite may also be written as $FeO \cdot Fe_2O_3$, which is one part wustite (FeO) and one part hematite (Fe_2O_3). This refers to the different oxidation states of the iron in one structure, not a solid solution. The XRD scanning from 10°-70° shows the lines (220) , (311), (400), (422), (511), and (440) at 2θ = 31.275°, 36.755°, 44.915°, 54.789, 57.695°, and 63.265°, respectively for Fe_3O_4.

Fig. 6 shows representative SEM images of the magnetite nano-particles and their thermally treated product. Estimation of the particle size appeared very difficult for the samples reported herein specially because of their extremely small dimension and inherent nature of agglomeration which is obvious due to high dipole-dipole interactions among the uncapped nano-particles. It can be found in SEM images that the particles are more or less spherical in nature having an average size of ~ 100 nm.

From the investigation of Raman spectra, shown in **Fig.8**, at room temperature, the spectrum of magnetite shows four out of the five theoretically predicted phonon bands at 668, 538, 306, and 193 cm^{-1}.. To assess the optical properties of highly diluted magnetite nanoparticles suspension (10^{-3} volume fraction), UV-VIS absorbance spectra were recorded on spectrophotometer in double beam mode, with deionized water as reference solvent. The magnetic nanoparticles were prepared through different capping agents. The magnetic nanoparticles coated with Perchloric acid (PA sample) exhibit an increased absorbance toward shorter wavelengths in comparison to the CA sample (magnetic nanoparticles coated with citric acid), while for longer wavelengths the CA sample exhibit an increased absorbance in comparison to PA sample as shown in **Fig.9**.

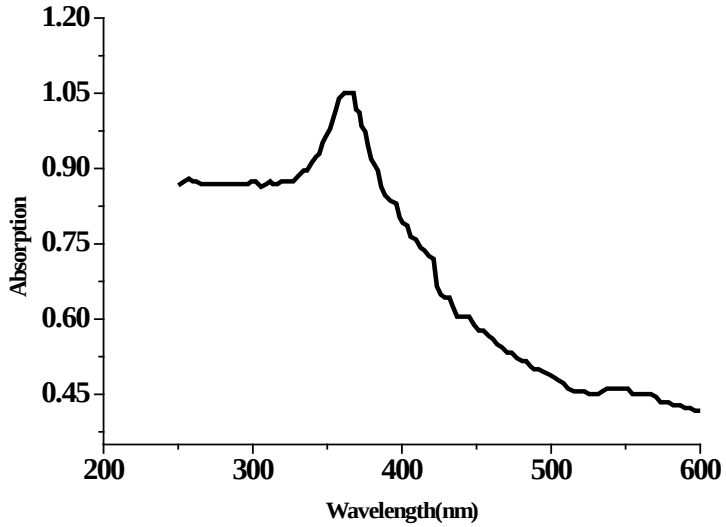

Fig. 4: UV absorption spectrum of ZnO sample

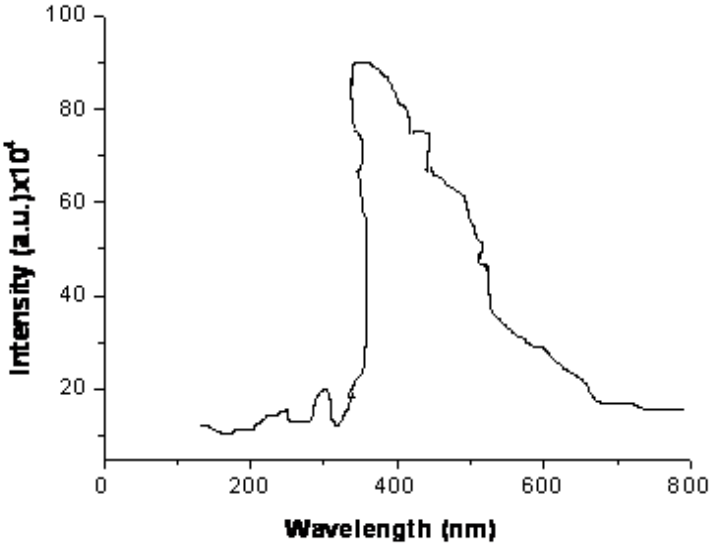

Fig. 5: PL spectrum of obtaining samples

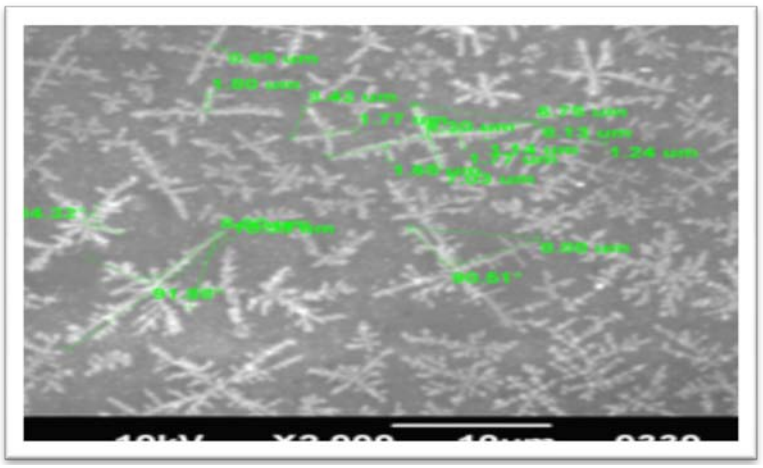

Fig. 6: SEM image of hematite NP at the different magnification

EDAX studies on the magnetite sample were carried out in a CARL-ZEISS EVO 50 XVP Low Vacuum Scanning Electron Microscope (LVSEM) -EDAX instrument equipped with Genesis 200 Energy Dispersive system which reveals that the elemental composition of the samples is Fe and O. **Fig. 7** represents the EDAX spectrum of the magnetite sample. Anal. calced (found) for Fe_3O_4: Fe, 72.36 (72.27); O, 27.64 (27.73) %.

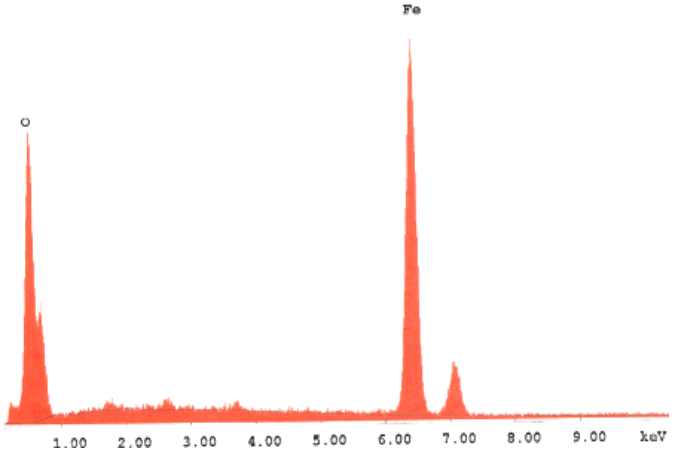

Fig. 7: EDAX spectrum of the magnetite nano-particles

Characterization of Polymer composite:
Conductivity measurement:

Nano crystals are found suitable for their large surface to bulk ratio giving wide interface area for dissociation into free charge carriers and their transportation. ZnO and Fe_3O_4 is a large band gap semiconductor like TiO_2 which is widely used in the different field. A solid solution of PVA and $LiClO_4$ is a familiar candidate for the creation of electrical double layer and considered as a promising battery material. **Fig.10 shows** the relationship between ion conductivity and Li salt concentrations for PVA - $LiClO_4$–ZnO, PVA - $LiClO_4$–ZnO and PVA - $LiClO_4$–ZnO-Fe_3O_4electrolytes.

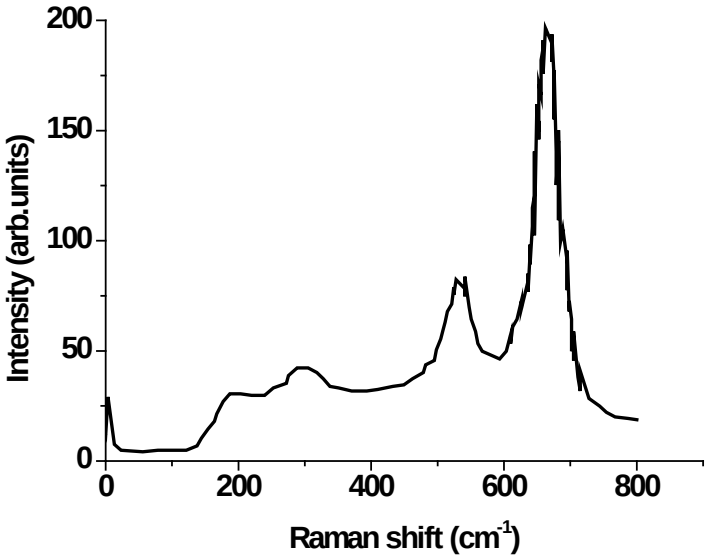

Fig. 8: Raman Spectra of Fe_3O_4nanoparticle

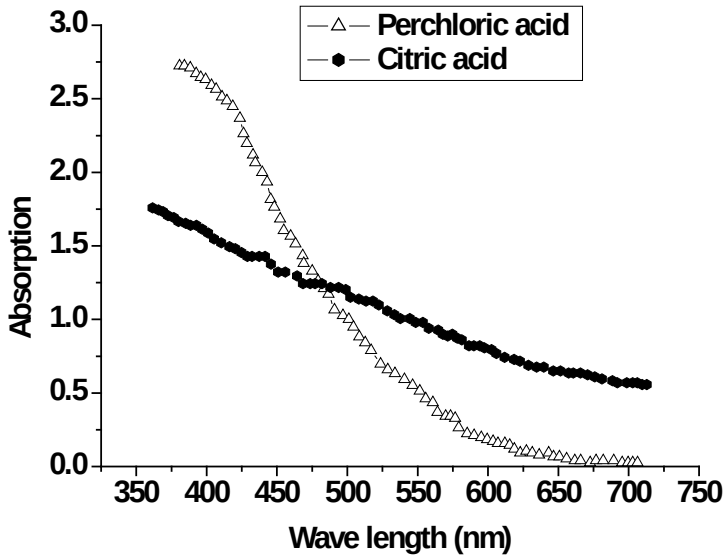

Fig. 9: UV-Vis spectra of magnetite nanoparticle

The electrolytes with 4 wt % reinforcing constituents showed conductivity of the order of 0.8-1.0 x10^{-4} S cm^{-1} at room temperature, while the PVA and $LiClO_4$-system without reinforcing materials showed a conductivity of below 0.1 x 10^{-4} S cm^{-1}.Conductivity of polymer electrolyte with reinforcement increases as a function of salt concentration very slowly at first, and exhibits a sharp increase at about 9 wt.% $LiClO_4$, followed by a sharp decline, while conductivity of electrolytes with 4wt.% ZnO, Fe_3O_4 and ZnO-Fe_3O_4 shows a steady increase and decrease. The possible reason may be because ZnO/and Fe_3O_4 particles enable plasticizing liquid to be loaded into the polymer electrolyte film by absorption. The maximum conductivity at specific ratios of polymer/Li-salt can be explained by the alteration of the carrier density and segmental motion (Doeff *et al*., 2000). The ionic conductivity increases with increasing lithium salt concentration due to the increase in the carrier density. However, the formation of ion-pairs becomes more serious in the case of high salt concentration than in the case of low concentration, leading to a drop in the ionic conductivity.

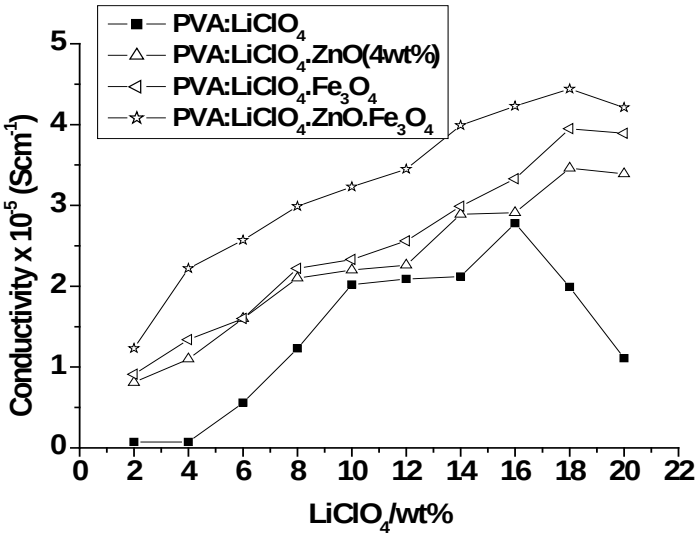

Fig. 10: Ionic conductivity of PVA–$LiClO_4$–ZnO-Fe_2O_3 electrolytes as a function of lithium salt content (at 25^0C).

The content of different nanopartices in the matrix also played an important role in conductivity. **Fig.11** shows the ionic conductivities of PVA–$LiClO_4$–ZnO, and PVA–$LiClO_4$–Fe_2O_3 electrolytes. The PVA

electrolyte with ZnO and Fe_2O_3 exhibit a maximum conductivity at ~11 wt % with ZnO and ~9 wt % for Fe_2O_3 respectively. Beyond the maximum, an addition of the reinforcing constituents decreases the ionic conductivity, probably due to the restriction of the ionic motion.

Impedance measurement:

Dispersion of ZnO and Fe_3O_4 nanoparticles in the host polymer enhanced the ionic conductivity. The nanoparticles assist ionic transport by increasing segmental mobility and interaction between Li+ ions and the polymer chains. In addition, the presence of ZnO and Fe_3O_4 nanoparticles in the polymer electrolyte alters the electrical potential distribution around the particle surface, which induces a space charge layer at the interface between the particles and the electrolyte. **Fig 12** is the complex membrane impedance spectrum (Nyquist Plot) of pure PVA and several PVA+10 what% $LiClO_4$ mixtures. The polymer composite shows the same nature, as shown in **Fig. 13.** By the doping of the nanoparticle inside the host lattice besides $LiClO_4$, the imaginary impedance drastically increases with the addition of reinforcing elements in the polymer matrix. The electrical conductivity is the ability of the material to conduct electricity. The resistance R offered by a conductor to the flow of the electric charge is found to be directly proportional to the length (l) and inversely proportional to the area of cross-section (A) of the conductor i.e.

$$R = \rho \frac{l}{A} \tag{3}$$

Where ρ is the proportionality constant and is called the electrical resistivity and the inverse of ρ is known as the electrical conductivity and is represented by σ. In another way, then σ may be defined as the proportionality constant in the linear relation of the current density (j) with the applied electric field gradient, such that (Samuel *et al* 2009)

$$J = \sigma E \tag{4}$$

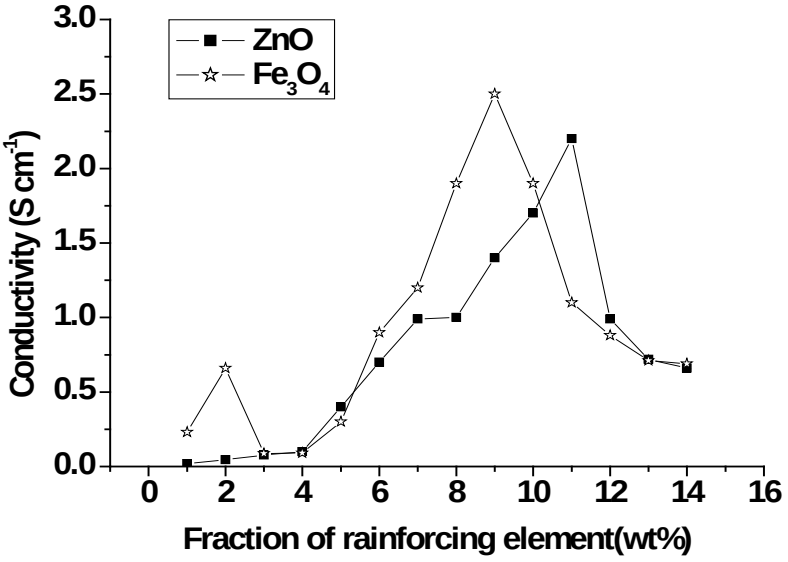

Fig. 11: Ionic conductivities of PVO–$LiClO_4$ (10 wt %) – Electrolytes as a function of ZnO and Fe_2O_3 content.

The magnitude of the electrical conductivity is determined by (i) the density of the charge carrier per unit volume (ii) charge carrier (iii) average drift velocity of the carrier per unit electric field. The charge carrier may be the electrons or ions, so the conductivity is either electronic or ionic. Further the nature of the binding of the agent with the parent polymer plays a vital role in determining the type of conductivity. $LiClO_4$ ionize in Li^+ and ClO_4^- in polymer electrolyte. This can be also enhanced with the addition of nanoparticle of ZnO and Fe_3O_4. Dispersion of ZnO and Fe_3O_4 nanoparticles in the host polymer enhanced the ionic conductivity. The nanoparticles assist ionic transport by increasing segmental mobility and interaction between Li+ ions and the polymer chains. In addition, the presence of ZnO and Fe_3O_4 nanoparticles in the polymer electrolyte alters the electrical potential distribution around the particle surface, which induces a space charge layer at the interface between the particles and the electrolyte. This may be due to interaction of Fe^{+2} and Fe^{+3} with ZnO nanoparticle

and with the polymer hole. The typical room temperature complex impedance spectrum of the polymer electrolyte PVA-$LiClO_4$ containing dispersed ZnO and Fe_3O_4 nanoparticles exhibiting maximum conductivity is shown **Fig 14**.

SEM investigation:

Fig.15 contains SEM images depicting the morphology of PVA, PVA-LiOH membranes with and without Fe_3O_4 nanoparticles. The morphology of the PVA membrane was uniform, and the surface roughness increased with increasing LiOH concentration However, the morphology of the membrane containing Fe_3O_4 nanoparticles was fragmented.

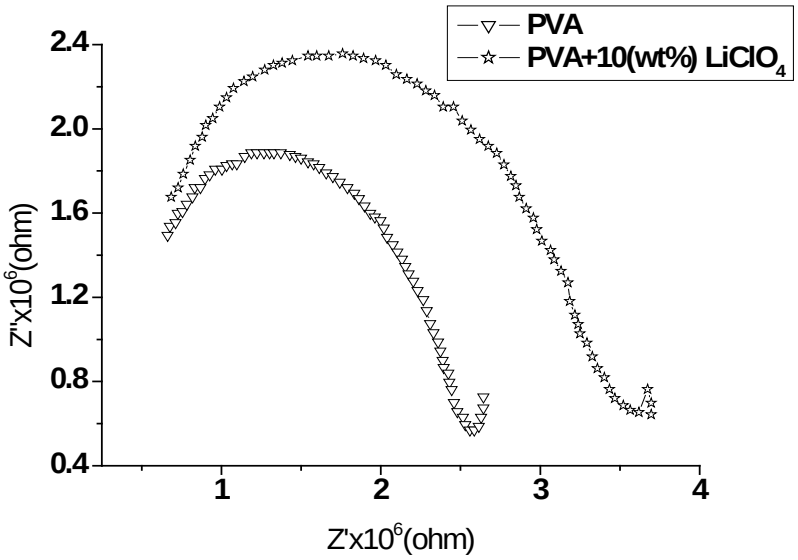

Fig. 12: Impedance spectrum and fitting curve for PVA.LiClO4 complex membrane polymer electrolyte at room temperature (a) 0 wt% (b) 10 wt%. $LiClO_4$

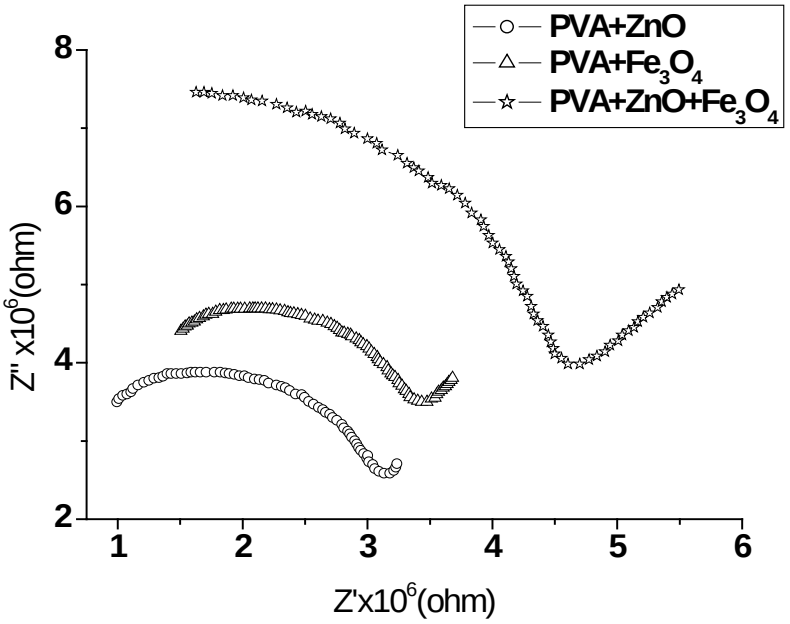

Fig. 13: Impedance spectrum and fitting curve for PVA $LiClO_4$(10 wt %) complex membrane polymer electrolyte at room temperature embedded with nanoparticle (~11 wt.% for ZnO and ~9 wt % for Fe_3O_4)

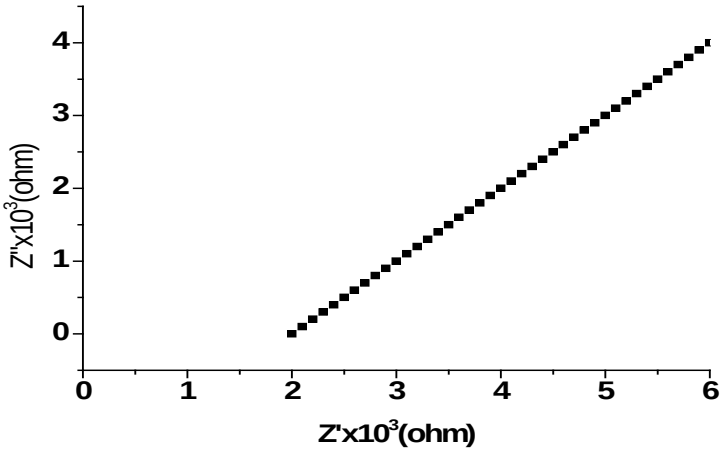

Fig. 14: Impedance spectrum of PVA.$LiClO_4$ containing dispersed ZnO and Fe_3O_4

The fragments may have been formed as the Fe_3O_4 nanoparticles filled the empty spaces between polymer chains. This is supported by the results of EDAX analysis indicating that the host polymer composition (C (72.02%), O (12.53%), FeO (9.06%)) and ZnO (6.39%) was retained in the nanoparticle-containing membranes. Fe_3O_4 particles synthesized in the absence of a polymer matrix possess an irregular morphology.

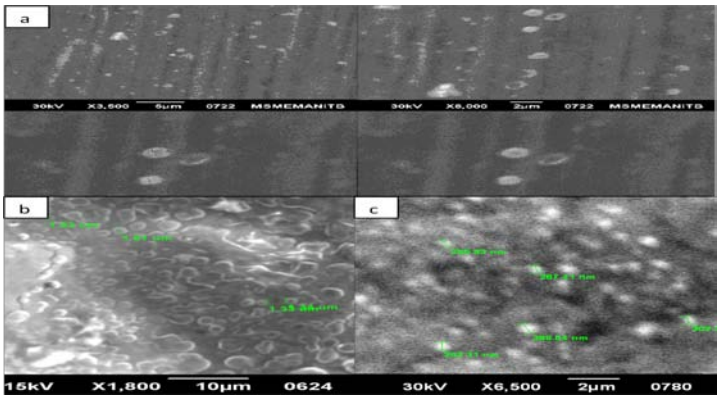

Fig. 15: SEM images of (a) PVA membrane, (b) 10wt% PVA.$LiClO_4$membrane, (c) and (d) 10wt% PVA.$LiClO_4$ containing ZnO-Fe_3O_4nanoparticles

Conclusion:

The following results are obtained from the present investigation:

1. The ZnO nano particles were synthesized from co-precipitation methods. The estimated size of the ZnO nano particles is approximately 32 nm.
2. The hematite nanoparticle was synthesized from precipitation method in alkaline media. The sizes of (hematite) Fe_3O_4 nanoparticle are approximately 100nm, because it is difficult to obtain the accurate sizes of hematite nanoparticles due to its inherent agglomeration properties. The best results are obtained when we used the capping agent.
3. From the UV-Visible investigation, the Zinc Oxide and Ferric oxide nanopartciles show the good absorbance capacities.
4. From the SEM investigation, the reinforcing constituents are uniformly distributed in the host matrix.
5. The dispersion of ZnO and Fe_2O_3 in PVA electrolyte enhances its electrical conductivity. The PVA electrolyte with ZnO and Fe_3O_4 exhibits a maximum conductivity (i.e., $1.81x10^{-3}$ S. cm^{-1}) at ~11 wt. % for ZnO and ~9wt % for Fe_3O_4.
6. Beyond the maximum, an addition of the reinforcing constituents decreases the ionic conductivity, probably due to the restriction of the ionic motion.
7. The impedance spectra of the composite material show a drastic change in impedance by the addition of the doping elements.

REFERENCE

Agrawal, S.L., M. Singh, M. Tripathi, M.M. Dwivedi and D.K. Pandey, 2009 .Dielectric relaxation studies on (PEO-SiO_2):NH_4SCN nanocomposite polymer electrolyte films. J. Mater. Sci., 44: 6060-6068.

Appetecchi, G.B., Y. Aihara, B. Scrosati, 2003. Investigation of Swelling Phenomena in Poly (ethylene oxide)-Based Polymer Electrolytes. *J. Electrochem. Soc.*, 150: A301.

Biswas, M., S.S. Ray, Y.P. Liu, 1999. Water dispersible conducting nanocomposites of poly (*N*-vinylcarbazole), polypyrrole and polyaniline with nanodimensional manganese (IV) oxide, Synth. Met., 105: 99.

Berger, P., B. Nicholas, Adelman, Katie J. Beckman, Dean J. Campbell, and Arthur B. Ellis. 199. Preparation and Properties of an Aqueous Ferrofluid. Journal of Chemical Education, 76(7).

Bruno, S., 2001. New approaches to developing lithium polymer batteries. *Chem. Record*, 1: 173.

Croce, F., G.B. Appetecchi, L. Persi and B. Scrosati, 1998. Nanocomposite polymer electrolytes for lithium batteries. Nature, 39: 456.

Croce, F., R. Curini, A. Martinelli, L. Persi, F. Ronci, B. Scrosati, R. Caminiti, 1999. Physical and chemical properties of nanocomposite polymer electrolytes", J. Phys. Chem. B, 103: 10632.

Doeff, M.M., L. Edman, S.E. Sloop, 2000. Transport Properties of Binary salt polymer electrolytes. J. Power Sources, 89: 227.

Hong, S.U., J. Won, Y.S. Kang, 2001. Polymer-salt complexes containing silver ions and their application to facilitated olefin transport membranes. Adv. Mater., 12: 968.

Kim, D.W., K.A. Noh, H.S. Min, D.W. Kang, Y.K. Sun, 2002. Porous Polyacrylonitrile Membrane for Lithium-Ion Cells. *Electrochem. Solid-State Lett.*, 5: A63.

Min, H.S., J.M. Ko, D.W. Kim2003. Preparation and characterization of porous polyacrylonitrile membranes for lithium-ion polymer batteries. J. Power Sources, 119: 469.

Pasquier, A. Du, P.C. Warren, D. Culver, A.S. Gozdz, G.G. Amatucci, J.M. Tarascon, 2000. Plastic PVDF-HFP electrolyte laminates prepared by a phase-inversion process. *Solid State Ionics*,135: 249.

Pesika, N.S., K.J. Stebe, P. C Searson, 2003, Determination of the particle size distribution of quantum nanocrystals from absorbance spectra. Adv. Matter., 15: 1289-1291

Ray, S.S., M. Biswas, 2000. Water-dispersible conducting nanocomposites of polyaniline and poly (*N*-vinylcarbazole) with nanodimensional zirconium dioxide, Synth. Met., 108: 231.

Ramesh, S., & A.K. Arof., 2001a. Ionic conductivity studies of plasticized poly (vinyl chloride) polymer electrolytes. Materials Science and Engineering B, 85: 11-15.

Saunier, J., F. Alloin, J.Y. Sanchez, R. Barriere, 2004. Plasticized microporous poly(vinylidene fluoride) separators for lithium-ion batteries. II. Poly (vinylidene fluoride) dense membrane swelling behavior in a liquid electrolyte—characterization of the swelling kinetics 2004, J. Polym. Sci., Part B: Polym. Phys., 42: 544.

Samuel, M.S., Lekshmi Bose, and K.C. George, 2009. Optical Properties of ZnO nanoparticle., XVI: 1&2: 57-65.

Su, S.J, N. Kuramoto, 2000. Processable polyaniline-titanium dioxide nanocomposites: effect of titanium dioxide on the conductivity, Synth. Met., 114: 147.

Wakihara, M., 2001. Recent Developments in lithium ion batteries *Mater.Sci. Eng. R*, 33: 109.

Weihua Pu, X., J. He, J. Li, C. Ying, C. Jiang, Wan, 2005. Controlled Crystallization of Spherical Active Cathode Materials for NiMH and Li-ion Rechargeable Batteries. Journal of New Materials for Electrochemical Systems, 8: 235-241.

Zhang, H.P., P. Zhang, Z. H. Li, M. Sun, Y.P. Wu, H.Q. Wu, 2007. A novel sandwiched membrane as polymer electrolyte for lithium ion battery *Electrochem.Commun.* 9: 1700,

Zhou Ji, Deshu Gao, Zhaohui Li, Gangtie Lei, Tiepeng Zhao, and Xiaohua Yi, 2010. Nanocomposite polymer electrolytes prepared by in situ polymerization on the surface of nanoparticles for lithium-ion polymer batteries" Pure Appl. Chem., 82(11): 2167-2174.